Circular dichroism in photoelectron spectroscopy of free chiral molecules: Experiment and theory on methyl-oxirane

S. Turchini,[1] N. Zema,[1] G. Contini,[1] G. Alberti,[2] M. Alagia,[3] S. Stranges,[3,4,5] G. Fronzoni,[6] M. Stener,[6] P. Decleva,[6] and T. Prosperi[1]

[1]*Istituto Struttura della Materia, CNR, Via Del Fosso del Cavaliere 100, 00133 Roma, Italy*

[2]*Istituto Metodologie Inorganiche e Plasmi, CNR, Sezione di Montelibretti, CP 10, 00016 Monterotondo Stazione, Italy*

[3]*Istituto per lo Studio dei Materiali Nanostrutturati, CNR, Sezione Roma 1, Piazzale A. Moro 5, 00185 Roma, Italy*

[4]*Dipartimento di Chimica, Università La Sapienza, P.le A. Moro 5, 00185 Roma, Italy*

[5]*Laboratorio TASC-INFM, Area Science Park, 34012, Basovizza (Trieste), Italy*

[6]*Dipartimento di Scienze Chimiche, Università di Trieste, Via L. Giorgieri 1, I-34127 Trieste, Italy and Consorzio Interuniversitario Nazionale per la Scienza e Tecnologia dei Materiali, INSTM, Unità di Trieste and INFM DEMOCRITOS National Simulation Center, Trieste, Italy*

(Received 21 January 2004; published 12 July 2004)

We report a joint experimental and theoretical study of circular dichroism in the valence photoelectron spectra of a free chiral molecule. The circular dichroism in photoelectron spectroscopy is measured at the magic angle for various valence states of $R(+)$ and $S(-)$ methyl-oxirane enantiomers in the vapor phase. The maximum dichroism measured is about 5×10^{-2}. Experimental and theoretical results are in agreement. The *ab initio* calculation employs a multicentric basis set of *B*-spline functions and a Kohn-Sham Hamiltonian.

DOI: 10.1103/PhysRevA.70.014502 PACS number(s): 31.15.Ar, 33.60.Cv, 33.55.Ad, 82.80.Pv

Natural circular dichroism (NCD) has contributed in the second half of the past century to the understanding of molecular stereochemistry in organic and inorganic compounds [1] and in the last decades much effort has been spent to extend the physical meaning and the experimental methods of the circular dichroism from visible to the vuv-x-ray wavelength range. The first measurement of the NCD in the x-ray range exploited the full power of the third generation synchrotron radiation circularly polarized insertion devices [2], which give high brilliance and well defined polarization rates. Few works are reported in the literature concerning NCD experiments in the vuv-soft x-ray energy range [3]. First asymmetry data in vuv photoelectron angular distribution has been recently measured in evaporated bromocamphor where the dichroism was found to be of the order of few percents [4]. The photoelectron signal (PE) measured is related to angle dependent photoionization intensity given by the following equation in case of circularly polarized light and random oriented molecules:

$$I(\theta)=\frac{\sigma(\omega)}{4\pi}\left[1-\frac{\beta(\omega)}{2}P_2(\cos\ \theta)+m_r D(\omega)P_1(\cos\ \theta)\right], \tag{1}$$

where σ is the cross section, β is the asymmetry parameter, and D is the dichroism parameter: these are dynamical quantities and their dependence on the photon energy ω is explicitly shown. In Eq. (1) P_i refers to the Legendre polynomial of ith degree, θ is the scattering angle between the photoelectron momentum and the light propagation, m_r is +1 or −1 for left and right circular polarization, respectively. We define left and right circularly polarized light according to the value $m_r=+1$ or $m_r=-1$ of the projection of the photon spin along its momentum. Accordingly, the electric vector describes a positive (right-handed) or negative (left-handed) screw. The photoelectron intensity along the θ direction shows different values not only in case of a change of the light helicity ($m_r=\pm1$) but also when, at fixed value of m_r, the photoelectron intensity is measured in forward/backward geometry, showing an asymmetry also in the angular distribution, according to the $\cos(\theta)$ dependence of the last term in Eq. (1). The angular resolved photoelectron spectroscopy (ARPES) with circular polarized light is therefore a very promising technique to detect chiral properties of molecules. The NCD in the angular distribution, shown in Eq. (1) is due to the dipole interaction term [5], while in the absorption process it is related to the second order interference terms, the electric dipole-electric quadrupole and electric dipole-magnetic dipole [6], the $(E1-E2)$ and $(E1-M1)$ mechanisms. Therefore, the circular dichroism in the photoelectron angular distribution (CDAD) is expected to be much more intense. The most compact way to give practical expressions to calculate the three dynamical parameters (σ, β, and D) which define the process is to recast the expressions of Chandra [7] employing the formalism of the angular momentum transfer [8]. The calculations of the dynamical parameters need the phase shifts (σ_1) and the dipole integrals $D^{(-)}_{lm}(\lambda_r)$ between the ionized orbital φ_i and the incoming wave normalized continuum $\varphi^{(-)}_{lm}$. The dipole integrals are calculated accordingly to Ref. [10] for each photoelectron kinetic energy value:

$$D^{(-)}_{lm}(\lambda_r)=\sqrt{\frac{4\pi}{3}}\langle\varphi^{(-)}_{lm}|rY_{1\lambda_r}|\varphi_i\rangle, \tag{2}$$

where in Eq. (2) λ_r indicates the three projection of the $l=1$ dipole vector operator. Such dipole integrals are transformed introducing a further angular momentum transfer l_t:

$$D^{l_t}_{lm}(\lambda_r) = (-1)^{l_t+m}(2l_t+1)^{1/2}\begin{pmatrix} 1 & l & l_t \\ -\lambda_r & m & \lambda_r - m \end{pmatrix} D^{(-)}_{lm}(\lambda_r), \tag{3}$$

which are employed to build the following product:

$$I(l_t,l,l') = \sum_{m\lambda_r m'\lambda'_r} D^{l_t}_{lm}(\lambda_r) D^{l_t}_{l'm'}(\lambda'_r)^* \delta_{m-\lambda_r,m'-\lambda'_r}. \tag{4}$$

From the quantities defined in Eq. (4) all the dynamical quantities split by angular momentum transfer contributions are obtained:

$$\sigma(l_t) = I(l_t,l_t+1,l_t+1) + I(l_t,l_t,l_t) + I(l_t,l_t-1,l_t-1), \tag{5}$$

$$\begin{aligned}\beta(l_t) = \{&(l_t+2)I(l_t,l_t+1,l_t+1) + (l_t-1)I(l_t,l_t-1,l_t-1) \\ &+ 3\sqrt{l_t(l_t+1)}[e^{i(\sigma_{l_t+1}-\sigma_{l_t-1})}I(l_t,l_t+1,l_t-1) + \text{c.c.}] \\ &- (2l_t+1)I(l_t,l_t,l_t)\}/(2l_t+1),\end{aligned} \tag{6}$$

$$\begin{aligned}D(l_t) = &\left\{[(-i)e^{i(\sigma_{l_t}-\sigma_{l_t-1})}I(l_t,l_t,l_t-1) + \text{c.c.}]\sqrt{\frac{l_t+1}{2l_t+1}}\right\} \\ &+ \left\{[(i)e^{i(\sigma_{l_t}-\sigma_{l_t+1})}I(l_t,l_t,l_t+1) + \text{c.c.}]\sqrt{\frac{l_t}{2l_t+1}}\right\},\end{aligned} \tag{7}$$

and from such partial contributions the $\sigma(\omega)$, $\beta(\omega)$, and $D(\omega)$ parameters which appear in Eq. (1) are finally obtained as sums of partial contributions:

$$\sigma(\omega) = \frac{4\pi^2\omega}{3c}\sum_{l_t}\sigma(l_t), \tag{8}$$

$$\beta(\omega) = \sum_{l_t}\beta(l_t)/\sum_{l_t}\sigma(l_t), \tag{9}$$

$$D(\omega) = \frac{3}{2}\left(\sum_{l_t} D(l_t)/\sum_{l_t}\sigma(l_t)\right). \tag{10}$$

From Eq. (7) it is evident that the D parameter will get nonzero contributions only when the quantities $I(l_t,l,l')$ from Eq. (4) will carry contributions of different parity, since $l = l' \pm 1$. In presence of inversion symmetry, states are classified accordingly to their parity (even or odd). Since the electric dipole operator is of odd parity, the continuum wave function will be of opposite parity with respect to the initial state, therefore only even or only odd l will contribute to the continuum and D will therefore be zero. With similar arguments, also in presence of a symmetry plane D must be zero: in fact consider the contributions to the sum (4), they are selected by the Kronecker symbol when $m-\lambda_r = m'-\lambda'_r$, each term has the counterpart $-m+\lambda_r = -m'+\lambda'_r$ which contributes to the sum and can be shown to be opposite in presence of a reflection plane, therefore in the sum there are only pairs of opposite sign which eliminate each other giving zero total contribution. To show that the contributions are opposite consider Eq. (3): when the sign of m and λ_r are changed the Wigner $3j$ symbol changes sign according to the parity of $1+l+l_t$, and since in Expression (7) $l=l_t$ and $l'=l_t+1$ there is always a difference of 1 between the parity of the dipoles and therefore their product will change sign. Of course the integral (2) is invariant by symmetry reflection and therefore the only sign change is due to the Wigner $3j$ symbol in Eq. (3).

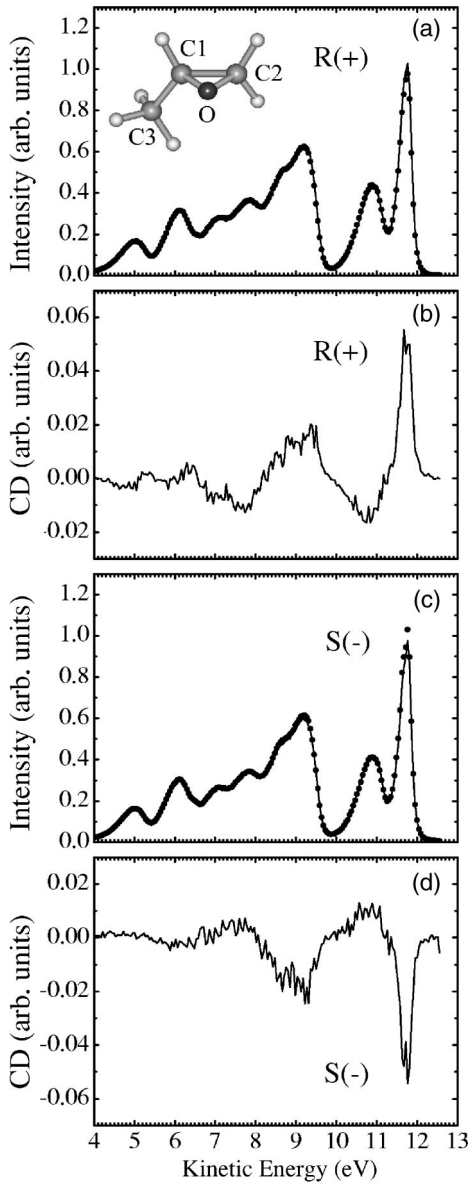

FIG. 1. Circular dichroism in the photoelectron spectra for methyl-oxirane in gas phase; (a),(c) photoelectron spectra for $R(+)$ and $S(-)$ methyl-oxirane obtained at 22.0 eV photon energy at the magic angle with right (solid line) and left (dots) circular polarized light; the inset shows a sketch structure of the $R(+)$ methyl-oxirane (C_3H_6O) molecule. (b),(d) dichroic ($I_+ - I_-$) spectra for $R(+)$ and $S(-)$ methyl-oxirane.

Pioneering calculations on the CDAD effects have been presented by Powis [9], who calculated rather strong dichroism for glyceraldehyde and lactic acid, up to 40% of the total intensity. However, the first experimental detection of the circular dichroism effects in the photoelectron spectra of bromocamphor has given a much smaller value, around 4% with

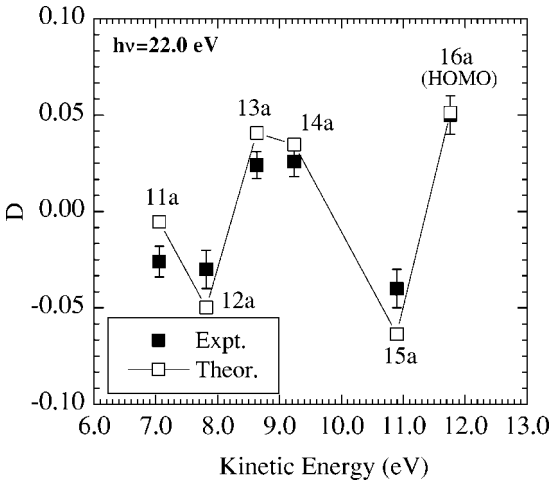

FIG. 2. Theoretical and experimental D parameters obtained at 22.0 eV photon energy for the valence photoionization channels of $R(+)$ methyl-oxirane.

respect to the total emission [4]. In order to better assess we have performed new theoretical calculations to describe the photoelectron continuum spectrum in large molecules without any approximation of the potential, employing a multicentric basis set of B-spline functions and a Kohn-Sham Hamiltonian, as described in detail in Ref. [10].

The experiment was performed at the circular polarization beamline at ELETTRA (Trieste) [11] which is downstream an electromagnetic elliptical wiggler/undulator [12] and is equipped with grazing and normal incidence (NIM) monochromators sharing the same entrance and exit slits. For this experiment the NIM was used at 22.0 eV with a resolving power $(E/\Delta E)$ of about 5000 and with a circular polarization rate of about 80%. The angle resolved photoelectron (PE) signals were obtained using the ARPES end station [13] equipped with twin hemispherical electron energy analyzers set at the magic angle $\theta_M = 54.7°$ with respect to the light propagation axis with 180° angle between them in forward-backward geometry. The effusive gas jet source was mounted perpendicular to both the photoelectron detection axes and the light propagation direction. The commercial methyl-oxirane liquid samples (optical isomers of 99% purity, raceme purity $>99.5\%$) were admitted through a needle at room temperature while gas pressure in the experimental chamber was kept constant at 1×10^{-3} Pa. In order to normalize the electron signals, the incident photon intensity was continuously measured after the ionization region with a photomultiplier tube and a phosphorous active surface. Total instrumental energy resolution, analyzer plus photon bandpass, was about 120 meV. The analyzer acceptance angle was ±3°. The transmission functions and kinetic energy calibrations of the two analyzers were systematically determined measuring the 3p photoemission in argon throughout the experiment. The validity of the experimental procedure, involving circular polarization switching to measure the dichroism parameter D, was checked by measuring the racemic sample. Methyl-oxirane is a good test molecule because of its conformational rigidity, that makes it suitable to extensive calculations, and monosigned dichroic absorption bands. The

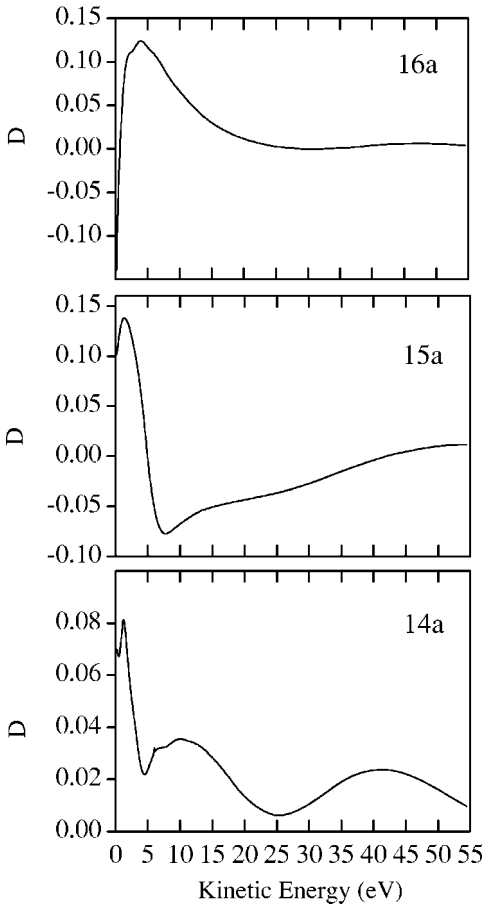

FIG. 3. Theoretical D parameters for the 16a, 15a, and 14a orbitals as a function of the kinetic energy of $R(+)$ methyl-oxirane.

valence PE spectra of the $S(-)$ and $R(+)$ enantiomers obtained at 22.0 eV photon energy are shown in Fig. 1 along with the measured dichroism. The spectra in the figure show all the expected eight valence states between 4 and 13 eV kinetic energy range investigated, in agreement with the published He I spectrum [14]. The dichroic spectrum, i.e., the difference between the photoelectron intensity with right and left circular polarized light, shows bands related one to one to the valence PE peaks. The enantiomers present mirror image dichroic spectra. The change of sign in the backward channel, as expected from Eq. (1), was also observed. Since *ab initio* calculations can provide dichroism parameters $D_i(\omega)$ for each photoionization channel, to compare experiment with theory it is crucial to extract the experimental D_i associated to each PE band from the peak intensity change measured on going from one circular polarization to the other by means of a fit procedure. To this purpose, asymmetric functions, obtained by a sum of Voigt components, were used to fit the valence PE spectra in order to take into account vibrational structures. The asymmetric functions thus obtained were used to fit the dichroic spectrum by leaving the amplitude as a free parameter, keeping fixed peak positions and widths. Different initial guesses compatible with the spectra were adopted to check the accuracy of the result and the numerical spread obtained is reported in the error bar along with the experimental D_i values. The data are corrected

for the polarization rate. In Fig. 2 the experimental and theoretical values of the dichroic parameters D_i of the $R(+)$ enantiomer are depicted for an excitation energy of 22 eV. Each value is related to a specific initial state ($16a-11a$) and kinetic energy. Figure 2 shows an overall excellent agreement between experiment and theory: the calculated D_i parameters reproduce both signs and orders of magnitude. A better agreement is observed in the high kinetic energy side; at low kinetic energy, also electron correlation plays a major role and a Kohn-Sham description, like the present one, may be less accurate in the energy region very near to the threshold. For orbitals in the range 4–6 eV, namely 10*a* and 9*a* states, the dichroism drops and the overall signal to noise ratio does not allow to have a well defined dichroic structure corresponding to these final states. We can estimate an upper limit for these structures of $D=\pm 0.02$. A simple Mulliken population analysis of the orbitals indicates that orbitals 16*a* and 15*a* are, respectively, ascribed to the oxygen lone pair and to a delocalized C–C, C–O, σ bond belonging to the oxirane ring, so they are, in first approximation, symmetric to a reflection with respect to the plane passing through the triatomic cycle, so the initial state has qualitatively a low degree of chirality. On the other hand the orbitals 14*a* and 13*a* have much stronger contribution from the CH_3 group which destroys the ring symmetry. To understand qualitatively more about the correlation between asymmetry, the sign and the strength of the *D* parameter it is useful to plot the calculated *D* parameters as a function of the photoelectron kinetic energy (Fig. 3). Actually we can identify different trends according to this qualitative discrimination: the 16*a* and 15*a* orbitals show an important structure in the *D* parameter very near the threshold, followed by a structureless tail, while the 14*a D* parameter is well modulated up to 50 eV. This may be an indication that for initial states of high chirality the *D* parameter gives structures at much higher energy. State 16*a* (HOMO) shows a very pronounced dichroic character, which decays rapidly with the energy. Calculation assigns to this state largely a 2*p* oxygen atomic character. Oxygen is a symmetric cromophore surrounded by a nonsymmetric environment represented by the triangular molecular plane made disymmetric by the presence only in one side of the methyl group. This finding suggests that the dichroism parameter *D* is not sensitive to the chirality of the initial orbital, but rather is able to map the whole molecular effective potential, i.e., the environment which contains the ionized orbital. This is not surprising due to the completely delocalized nature of the scattered photoelectron continuum orbital.

In conclusion, the circular dichroism in photoelectron spectroscopy on randomly oriented chiral molecules gives the opportunity to have, via the odd–even mixing of the wave function, a fingerprint of the interplay between asymmetry and electronic properties. The circular dichroism effect in photoelectron spectroscopy is very sensitive to the electronic structure of the system as demonstrated by the rich and various shapes exhibited by *D* parameters obtained for different orbitals. The effect is accurately reproduced at the theoretical level employing the *B*-spline DFT method, which appears valuable in the prediction of the effect and interpretation of the experiment.

This work has been supported by grants from MIUR (Programmi di Ricerca di Interesse Nazionale COFIN ex 40%) of Italy and CNR of Rome (Italy). An INSTM grant of computer time on the IBM SP4 of CINECA (Bologna, Italy) is gratefully acknowledged.

[1] S. F. Mason, *Molecular Optical Activity and the Chiral Discriminations* (Cambridge University Press, Cambridge, 1981).
[2] L. Alagna, T. Prosperi, S. Turchini, J. Goulon, A. Rogalev, C. Goulon-Ginet, C. R. Natoli, R. D. Peacock, and B. Stewart, Phys. Rev. Lett. **80**, 4799 (1998).
[3] S. Turchini, N. Zema, S. Zennaro, L. Alagna, B. Stewart, R. D. Peacock, and T. Prosperi, J. Am. Chem. Soc. (in press).
[4] N. Böwering, T. Lischke, B. Schmidtke, N. Müller, T. Khalil, and U. Heinzmann, Phys. Rev. Lett. **86**, 1187 (2001).
[5] B. Ritchie, Phys. Rev. A **13**, 1411 (1976).
[6] L. D. Barron, Mol. Phys. **21**, 241 (1971); Y. N. Chiu, J. Chem. Phys. **52**, 1042 (1970).
[7] N. Chandra, J. Phys. B **20**, 3405 (1987).
[8] U. Fano and D. Dill, Phys. Rev. A **6**, 185 (1972).
[9] I. Powis, J. Chem. Phys. **112**, 301 (2000).
[10] D. Toffoli, M. Stener, G. Fronzoni, and P. Decleva, Chem. Phys. **276**, 25 (2002).
[11] Desiderio *et al.*, Synchrotron Radiat. News **12**, 34 (1999).
[12] R. P. Walker and B. Diviacco, Rev. Sci. Instrum. **63**, 332 (1992).
[13] R. R. Blyth *et al.*, J. Electron Spectrosc. Relat. Phenom. **101-103**, 959 (1999).
[14] K. Kimura, S. Katsumata, Y. Achiba, T. Yamazaki, and S. Iwata, *Handbook of HeI Photolectron Spectra of Fundamental Organic Compounds* (Japan Scientific Society, Tokyo, 1981).